Entropic sampling via Wang-Landau random walks in dominant energy subspaces

A. Malakis,* S. S. Martinos, I. A. Hadjiagapiou, N. G. Fytas, and P. Kalozoumis
Department of Physics, Section of Solid State Physics, University of Athens, Panepistimiopolis, GR 15784 Zografos, Athens, Greece
(Received 21 July 2005; revised manuscript received 4 November 2005; published 22 December 2005)

Dominant energy subspaces of statistical systems are defined with the help of restrictive conditions on various characteristics of the energy distribution, such as the probability density and the fourth order Binder's cumulant. Our analysis generalizes the ideas of the critical minimum energy subspace (CRMES) technique, applied previously to study the specific heat's finite-size scaling. Here, we illustrate alternatives that are useful for the analysis of further finite-size anomalies and the behavior of the corresponding dominant subspaces is presented for the two-dimensional (2D) Baxter-Wu and the 2D and 3D Ising models. In order to show that a CRMES technique is adequate for the study of magnetic anomalies, we study and test simple methods which provide the means for an accurate determination of the energy–order-parameter (E,M) histograms via Wang-Landau random walks. The 2D Ising model is used as a test case and it is shown that high-level Wang-Landau sampling schemes yield excellent estimates for all magnetic properties. Our estimates compare very well with those of the traditional Metropolis method. The relevant dominant energy subspaces and dominant magnetization subspaces scale as expected with exponents α/ν and γ/ν, respectively. Using the Metropolis method we examine the time evolution of the corresponding dominant magnetization subspaces and we uncover the reasons behind the inadequacy of the Metropolis method to produce a reliable estimation scheme for the tail regime of the order-parameter distribution.

DOI: 10.1103/PhysRevE.72.066120 PACS number(s): 05.50.+q, 64.60.Cn, 64.60.Fr, 75.10.Hk

I. INTRODUCTION

Computer simulations based on Monte Carlo sampling methods have increased dramatically our understanding of the behavior of the standard classical statistical mechanics systems (for instance Ising-like models), but also of more complex systems, such as disordered media and polymeric and glassy materials. Our main approach, in the past half century, was based on importance sampling in the canonical ensemble. The Metropolis method and its variants were, for many years, the main tools in condensed matter physics, particularly for the study of critical phenomena [1–5]. However, for complex systems effective potentials have a complicated rugged landscape with many minima and maxima which become more pronounced with increasing system size. In many such cases the Metropolis method and its variants are very inefficient methods. Entropic sampling methods (ESMs) are alternatives to the importance sampling methods, which at least in principle do not suffer from such problems. Of course, for second order phase transitions in unfrustrated systems cluster algorithms are quite efficient and have essentially solved the "critical slowing down" problem. The performance limitations of flat-histogram or entropic methods have recently attracted considerable interest. Even for simple systems, such as the Ising model, such methods have tunneling times in energy space that are not proportional to N^2 as should be expected for a pure random walk, but they are proportional to a higher power. Moreover, it has been shown that tunneling times may be strongly dependent on the model under consideration [6]. Furthermore, in order to apply an ESM the density of states (DOS) of the system should be known.

Over the last decade, several efficient methods that directly calculate the DOS of classical statistical models have been developed. A few remarkable examples are the entropic [5,7], multicanonical [8], broad histogram [9,10], transition matrix [11], and Wang-Landau [12] methods. Using these methods, it is now possible to accurately estimate the DOS of quite large classical statistical models [13]. Since for complex systems the Metropolis method may be trapped for very long times in nonrepresentative energy subspaces it is reasonable to consider an ESM program using an approximate DOS as an alternative to the traditional importance sampling methods. Although this idea exists in the literature [4], the effectiveness of the various possible implementations has not been exploited by systematic comparative studies. For instance, the following two-run strategy may be used in an ESM program. In the first stage an accurate estimation of the DOS of the system under consideration is achieved with the help of, say, the Wang-Landau (WL) method, and in the second stage the derived DOS is used in an ESM to estimate further properties of the system, such as the order-parameter distribution. In such a two-stage program, the critical minimum energy subspace (CRMES) method recently developed by Malakis *et al.* [14,15] may be used to restrict the energy space and make such a program more efficient for the estimation of the critical behavior of any statistical system. Our first objective in this paper is to extend the CRMES condition and to observe to what degree appropriately defined energy subspaces are sufficiently large for the estimation of all finite-size anomalies. Our second objective focuses on the possibility to obtain all critical properties of the system by using a one-run strategy of an ESM, based on a WL random walk in a restricted energy subspace.

The rest of the paper is organized as follows. In Sec. II we provide a brief outline of the CRMES restriction and give alternative definitions of the dominant energy subspaces. The

*Corresponding author. Electronic address: amalakis@cc.uoa.gr

scaling of the extensions of these subspaces is illustrated for the Baxter-Wu and Ising models. In Sec. III A we discuss how, by employing the WL and the N-fold implementation of the WL scheme in a restricted energy subspace, we may generate approximations of the DOS of the system and at the same time obtain energy–order-parameter (E,M) histograms. It is suggested that this one-run WL strategy yields good estimates of all magnetic properties. In Sec. III B we consider the two-dimensional (2D) Ising model as a test case. Our estimates are compared with those of the traditional Metropolis method and the expected magnetic scaling behavior is recovered. Finally, in Sec. III C we study our dominant subspace method in the energy and the order-parameter space. The subspaces sufficient for an accurate estimation of magnetic finite-size anomalies are determined and their scaling is analyzed. The tail regime of the order-parameter critical distribution is briefly discussed and the shortcomings of the Metropolis method are clarified. Our conclusions are summarized in Sec. IV.

II. ALTERNATIVES FOR RESTRICTING THE ENERGY SPACE

Let us start by recalling the original CRMES restriction of Malakis *et al.* [14]. Assume that $\tilde{E}$ denotes the value of energy producing the maximum term in the partition function of the statistical model, for instance the Ising model, at some temperature of interest. Since we deal with a finite system of linear size L, we are interested in the properties (finite-size anomalies) near some pseudocritical temperature T_L^*, which in general depends on L but also on the property studied. Thus, for the specific heat peaks let us use the notation $T_L^*[C] \equiv T_{L,C}$ for the pseudocritical temperature and define a set of approximations by restricting the statistical sums to energy subranges around the value $\tilde{E}=\tilde{E}(T_L^*[C])=\tilde{E}(T_{L,C})$. Let these subranges of the total energy range (E_{min},E_{max}) be denoted as follows:

$$(\tilde{E}_-,\tilde{E}_+), \quad \tilde{E}_\pm = \tilde{E} \pm \Delta^\pm, \quad \Delta^\pm \geqslant 0. \tag{1a}$$

Accordingly, the peaks are approximated by

$$C_L(\tilde{E}_-,\tilde{E}_+) \equiv C_L(\Delta^\pm) = N^{-1}T^{-2}\left[\tilde{Z}^{-1}\sum_{\tilde{E}_-}^{\tilde{E}_+} E^2 \exp[\tilde{\Phi}(E)] - \left(\tilde{Z}^{-1}\sum_{\tilde{E}_-}^{\tilde{E}_+} E \exp[\tilde{\Phi}(E)]\right)^2\right], \tag{1b}$$

$$\tilde{\Phi}(E) = [S(E) - \beta E] - [S(\tilde{E}) - \beta \tilde{E}], \quad \tilde{Z} = \sum_{\tilde{E}_-}^{\tilde{E}_+} \exp[\tilde{\Phi}(E)]. \tag{1c}$$

Since by definition $\tilde{\Phi}(E)$ is negative we can easily see that for large lattices extreme values of energy (far from $\tilde{E}$) will have an extremely small contribution to the statistical sums, since these terms decrease exponentially fast with the distance from $\tilde{E}$. It follows that, if we request a specified accuracy, then we may restrict the necessary energy range in which DOS should be sampled. To introduce the minimum energy subspace (MES), we impose the condition

$$\left|\frac{C_L^*(\Delta_\pm)}{C_L^*} - 1\right| \leqslant r, \tag{2}$$

where r measures the relative error and it will be set equal to a small number $(r=10^{-6})$, and C_L^* is the value of the maximum of the specific heat obtained by using the total energy range. With the help of a convenient definition, we can specify the minimum energy subspaces satisfying the above condition. Their finite-size extensions will be denoted by:

$$(\Delta\tilde{E})_C \equiv (\Delta\tilde{E})_{C_L^*,r} \equiv \min(\tilde{E}_+ - \tilde{E}_-). \tag{3}$$

Demanding the same level of accuracy (r) for all lattice sizes, we produce a size dependence on all parameters of the above energy ranges and in particular the extensions of the critical MES should obey the scaling law [14]

$$\Psi_C \equiv \frac{(\Delta\tilde{E})_C^2}{L^d} \approx L^{\alpha/\nu}. \tag{4}$$

In order to determine the location of the MES we may follow successive minimal approximations to the specific heat peak [14]:

$$C_L(j) \equiv C_L(\Delta_j^-,\Delta_j^+), \quad \Delta_{j+1}^\pm = \Delta_j^\pm \pm \theta_{j+1}^\pm, \quad \Delta_1^\pm = 0, \tag{5a}$$

$$j = 1,2,\ldots,$$

where one of the above θ increments is chosen to be 1 and the other 0 according to which side of $\tilde{E}$ is producing at the current stage the best approximation:

$$(\theta_{j+1}^+ = 1, \theta_{j+1}^- = 0) \Leftrightarrow |C_L - C_L(\Delta_j^-,\Delta_j^+ + 1)| \leqslant |C_L - C_L(\Delta_j^- + 1,\Delta_j^+)|,$$

$$(\theta_{j+1}^+ = 0, \theta_{j+1}^- = 1) \Leftrightarrow |C_L - C_L(\Delta_j^-,\Delta_j^+ + 1)| > |C_L - C_L(\Delta_j^- + 1,\Delta_j^+)|. \tag{5b}$$

The above defines a sequence of relative errors for the specific heat peaks (r_j):

$$r_j = \left|\frac{C_L(j)}{C_L^*} - 1\right|, \tag{5c}$$

and the MES is the subspace centered at $\tilde{E}$ corresponding to the first member of the above sequence (5) satisfying $r_j \leqslant r$. The location of these subspaces can be predicted either by extrapolation, from smaller lattices, or by using the early-stage DOS approximation of the WL method [15]. Using a sufficiently wider subspace we can also accurately estimate their extensions and verify the scaling law (4) as shown in Ref. [14].

The above scheme has been tested for the Ising and Baxter-Wu models [14,15] and it has been shown that this

particular rule provides very accurate extensions satisfying quite well the expected scaling law (4). However, one may conceive other ways for specifying the locations of the energy subspaces that will essentially produce comparable approximations. A simple idea is to use a condition based on the energy probability density $[f_{T_{L,C}^*}(E) \propto \tilde{\Phi}(E)]$ meaning the application of Eq. (6) at a particular pseudocritical temperature $T_{L,C}$. That is, we may define the end points $(\tilde{E}_{\pm})$ of the subspaces by simply comparing the corresponding probability densities with the maximum at the energy $\tilde{E}$:

$$\tilde{E}_{\pm}: \quad \exp\{\tilde{\Phi}(\tilde{E}_{\pm})\} \leqslant r. \tag{6}$$

Applying this restriction at a particular (pseudocritical) temperature (T_L^*) is much easier than applying the successive minimal approximations described in Eq. (5) and it will produce comparable approximations for the specific heat maxima. The corresponding scaling variable $\Psi_{f_{T_{L,C}^*}(E)}$ for the resulting MES should also obey the law (4). Another interesting pseudocritical temperature is the temperature corresponding to the fourth order Binder's cumulant for the energy distribution. This reduced cumulant is defined by

$$V_L(T) = 1 - \frac{\langle E^4 \rangle}{3\langle E^2 \rangle^2} \tag{7}$$

and it is well known [15–17] that this quantity has a minimum V_L^* at a pseudocritical temperature $T_L^*[V] \equiv T_{L,V}$. In the thermodynamic limit this temperature also approaches the critical temperature but for finite lattices is different from the pseudocritical temperature $T_{L,C}$ of the specific heat. Thus, the maximum term of the partition function, corresponding to the temperature of the cumulant finite-size anomaly, will be now located at a different value of the energy spectrum [say, at $\tilde{E}(T_{L,V})$]. Therefore, if we follow the probability density criterion described above in Eq. (6) to define the CRMES at these temperatures we will generally find subspaces that do not coincide with the subspaces for the specific heat. However, for large lattices the nonoverlapping parts of these subspaces are relatively very small and we may run the WL algorithm in the union of these subspaces in order to study both properties.

Let us now follow an analogous approach with the successive minimal approximations of Eq. (5) for the cumulant anomaly. It is of interest to note that if we define the CRMES by a similar condition

$$\left| \frac{V_L^*(\Delta_{\pm})}{V_L^*} - 1 \right| \leqslant r \tag{8}$$

then, for sufficiently large lattices, the scaling law (4) for the corresponding extensions [we may now use the $\Psi_V = (\Delta\tilde{E})_V^2 / L^d$ variable] will not be obeyed. This is due to the fact that the cumulant goes asymptotically to a finite value $(V_\infty^* = V_\infty = 2/3)$ and therefore the relative accuracy criterion (8) is not appropriate for large lattices or, in other words, becomes ineffective (see also the discussion bellow). We may now introduce the finite-size distance from the asymptotic value of the Binder parameter, $(V_\infty^* - V_L^*)$, to our considerations and modify the criterion (8) as follows:

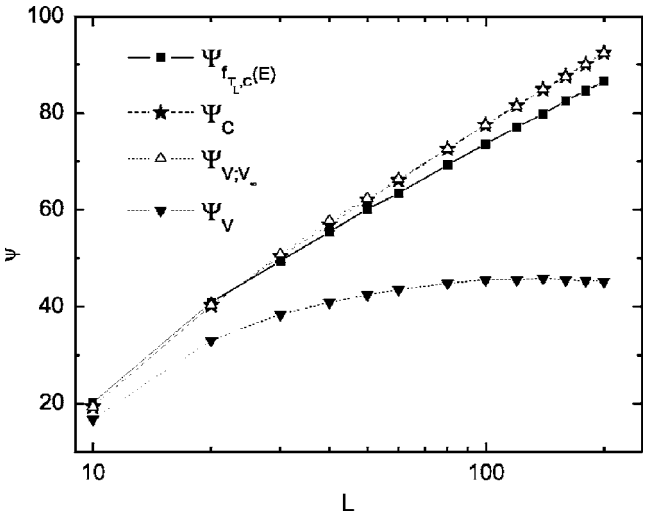

FIG. 1. 2D Ising model ($L=10-100$ [14], $L=120,140,\ldots,200$ this work). Behavior of scaling variables corresponding to various alternative definitions of dominant energy subspaces defined in the text. $\Psi_{f_{T_{L,C}^*}(E)}$ is the scaling variable defined with the help of the restriction (6) at the pseudocritical temperature $T_{L,C}$. Correspondingly, Ψ_C is the scaling variable defined from Eq. (5) at the pseudocritical temperature $T_{L,C}$ and $\Psi_{V;V_\infty}$ is the scaling variable defined from Eq. (9) at the pseudocritical temperature $T_{L,V}$. Finally, Ψ_V is the scaling variable defined from Eq. (8) at the pseudocritical temperature $T_{L,V}$. Note the strong decline of this last variable from the expected asymptotic law, as explained in the text. The logarithmic scale in the x axis is used in order to facilitate the observation of the logarithmic behavior.

$$\left| \frac{V_L^*(\Delta_{\pm})}{V_L^*} - 1 \right| \Bigg/ \left| \frac{V_L^*}{V_\infty^*} - 1 \right| \leqslant r. \tag{9}$$

It appears (see below) that this option makes the extensions of the resulting subspaces follow very well the scaling law (4) and for the 2D Ising model we obtain an almost perfect coincidence with the extensions of the corresponding subspaces obtained for the specific heat. The corresponding scaling variable will be denoted by $\Psi_{V;V_\infty} = (\Delta\tilde{E})_{V;V_\infty}^2 / L^d$. For a second order transition the limiting value of the energy cumulant is known $(V_\infty^* = 2/3)$ and this makes the implementation of the scheme (9) possible.

The above alternative definitions for the CRMES were applied to the 2D Ising model using the DOS data of Ref. [14] ($L=10-100$) but also additional data up to $L=200$ ($L=120,140,160,180,200$). Figure 1 illustrates the scaling behavior of the corresponding scaling variables for the CRMES of the specific heat at its pseudocritical temperature $T_{L,C}$ using the minimum subspaces resulting from Eq. (5c), and also the minimum subspaces resulting, at this temperature, from the probability density condition studied in Eq. (6). The same figure displays the estimates for the two options (8) and (9) for the CRMES corresponding to the minimum of the Binder parameter at its pseudocritical temperature $T_{L,V}$. The expected logarithmic scaling law [14,18] is obeyed well for all

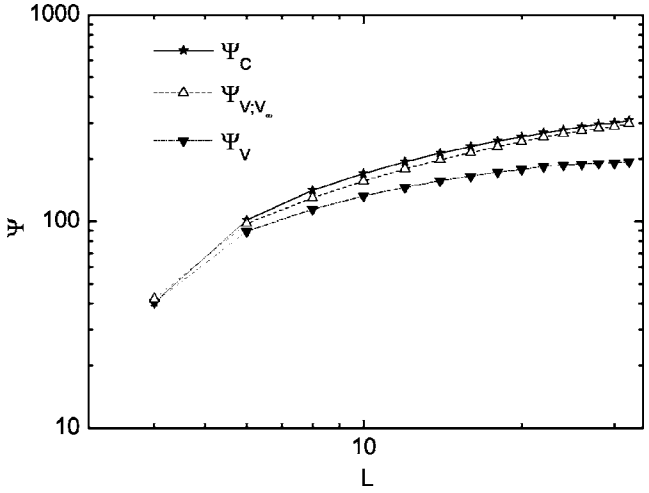

FIG. 2. 3D Ising model ($L=4-32$ [14]). Behavior of the scaling variables Ψ_C, $\Psi_{V;V_\infty}$, and Ψ_V, as in Fig. 1. Note again the clear decline of the variable Ψ_V, defined by Eq. (8). The log-log scale is used in order to observe the expected power law.

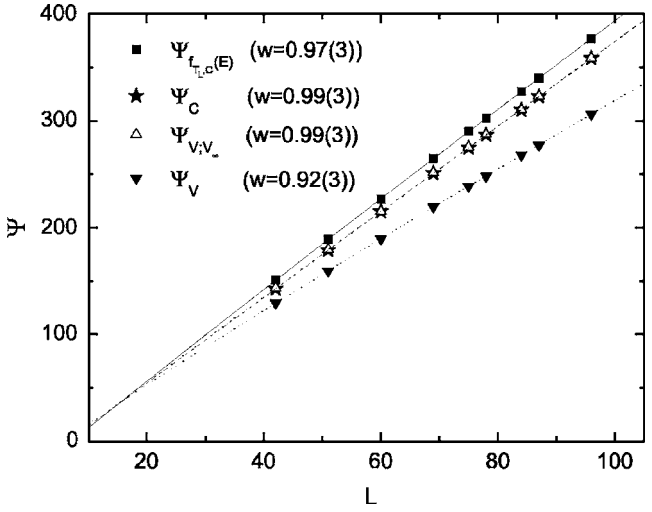

FIG. 3. 2D Baxter-Wu model ($L=42$, 51, 60, 69, 75, 78, 84, 87, and 96 [15]). Behavior of the scaling variables $\Psi_{f_{T^*_L,C}(E)}$, Ψ_C, $\Psi_{V;V_\infty}$, and Ψ_V, again as in Fig. 1. The modest decline of the variable Ψ_V defined in Eq. (8) is due to the fact that the cumulant minimum is much deeper for this model. The fitted lines correspond to power laws of the form $\Psi=a+bL^w$ with exponents $w=0.97(3)$, 0.99(3), 0.99(3), and 0.92(3), respectively. The finest estimate for the expected critical exponent $w=\alpha/\nu=1$ is the one corresponding to the original definition [Eqs. (2)–(5)] of the minimum subspaces.

definitions with the clear exception of the cumulant condition (8) in which case the scaling variable shows a clear decline from the logarithmic divergence for large lattices. This is due to the fact that this parameter approaches the finite value $V^*_\infty=2/3$, and the condition defined in Eq. (8) becomes ineffective for large lattices. Note that with increasing lattice size several significant figures of this finite number are determined from a small part of the dominant energy subspace. The trick proposed in Eq. (9) not only keeps the scheme in the proper scaling form but also is remarkable in that the resulting extensions of the CRMES of the specific heat and the Binder parameter completely coincide for the 2D Ising model. This coincidence occurs also for the Baxter-Wu model, but not for the 3D Ising model (see below). Note, however, that the corresponding pseudocritical temperatures are different and their CRMESs do not coincide (for $L=100$ their displacement is 20 energy levels), only their extensions are equal. Figure 2 illustrates the behavior of the same scaling variables for the 3D Ising model using the DOS data of Ref. [14]. The situation is very similar and is described by the power law (4) as discussed in Ref. [14]. It is noteworthy that the cumulant condition (8) leads to a clear decline from the appropriate power law for large lattices and the trick proposed in Eq. (9) seems to yield the expected critical behavior. Finally, Fig. 3 presents the analogous graphs for the Baxter-Wu model using the DOS data of [15]. Again the scaling variables appear to follow the expected scaling law (4) and a decline in the case of the condition (8) is observed. However, this decline is weaker for the Baxter-Wu model due to the fact that the cumulant minimum is quite deeper for this model, that is, the difference $(V^*_\infty - V^*_L)$ is relatively larger for the Baxter-Wu model. Fitting these data to the expected power law (see the discussion in the caption of Fig. 3) we find that the best estimate for the exponent α/ν is produced from the original [14,15] minimum subspaces of the specific heat. As mentioned above the extensions of the CRMES determined for the cumulant by the condition (9) for the 2D Baxter-Wu model coincide with the extensions of the CRMES of the specific heat [Eq. (2)] of the model.

III. ENTROPIC SAMPLING VIA WL RANDOM WALKS

A. Microcanonical estimators via the WL scheme

As mentioned in the Introduction, the ESM using an exact (if available) or an accurate approximation of the DOS may be considered as an alternative to the various importance sampling methods used in the literature to estimate canonical averages and probability distributions of macroscopic thermodynamic variables. Here we shall examine the idea of producing accurate estimates for finite-size magnetic anomalies by using a simple ESM based on the WL random walk in an appropriately restricted energy subspace (E_1,E_2). We shall also test our results by comparing to the Metropolis method [1].

We implement a WL random walk in a restricted energy subspace (E_1,E_2) and at the same time we accumulate data for the two-parameter (E,M) histogram. For a large system we employ a multirange algorithm [12] in which independent random walks are used for different energy subintervals and the resultant pieces are then combined to obtain the DOS in (E_1,E_2). The WL modification factor (f_j) is reduced at the jth iteration according to $f_1=e$, $f_j \rightarrow f_{j-1}^{1/2}$, $j=2,\ldots,J_{fin}$ and for the histogram flatness we use a 5% criterion as in our previous studies [14,15,19]. Note that the detailed balance condition is satisfied in the limit $f \rightarrow 1$. Let the exact density of states be denoted by $G(E)$ and the DOS of the above WL process be denoted by $G_{WL}(E)$. Similarly, let $H_{WL}(E,M)$ be the histogram produced during the WL process by a specific recipe which will be described below.

The resulting approximation of the DOS and the corresponding E,M histograms may be used to estimate the magnetic properties of the system in a temperature range that is covered by the restricted energy subspace (E_1,E_2). Canonical averages will be then approximated as follows:

$$\langle M^n\rangle = \frac{\sum_E \langle M^n\rangle_E G(E) e^{-\beta E}}{\sum_E G(E) e^{-\beta E}} \cong \frac{\sum_{E\in(E_1,E_2)} \langle M^n\rangle_{E,WL} G_{WL}(E) e^{-\beta E}}{\sum_{E\in(E_1,E_2)} G_{WL}(E) e^{-\beta E}} \tag{10a}$$

where the microcanonical averages $\langle M^n\rangle_E$ are obtained from the $H_{WL}(E,M)$ histograms as

$$\langle M^n\rangle_E \cong \langle M^n\rangle_{E,WL} \equiv \sum_M M^n \frac{H_{WL}(E,M)}{H_{WL}(E)}, \tag{10b}$$

$$H_{WL}(E) = \sum_M H_{WL}(E,M),$$

and the summation in M runs over all values generated during the process in the restricted energy subspace (E_1,E_2).

The accuracy of the magnetic properties obtained from the above averaging process will depend on many factors. First, the energy subspace used restricts the temperature range for which such approximations may be accurate. This restriction has as a result that the process will not visit all possible values of M, but this fact is of no consequence for the accuracy of the magnetic properties at the temperature range of interest, as long as the estimated DOS is accurate. Second, the accuracy of the above microcanonical estimators will, as usual, depend on the total number of visits to a given energy level $[H_{WL}(E)]$, and also on the number of different spin states visited within this energy level. However, these are statistical fluctuations inherent in any Monte Carlo method and we should expect improvement by increasing the number of repetitions of the process. At this point let us note that statistical fluctuations may be reduced, as usually, by multiple measurements but also by using some refinements of the original WL algorithm [20,21]. An illustrative figure including such a refinement will be presented in the next subsection. Finally, the construction of reliable (uniform) approximations for microcanonical averages is an important open problem, discussed recently in some detail by Oliveira [22]. The microcanonical approximations ($\langle M^n\rangle_{E,WL}$) appearing in Eq. (10) and used in this paper are obtained from the WL multirange process, and the corresponding N-fold version of Shulz *et al.* [23]. The recipes employed are outlined and tested in the following.

There are mainly three categories of microcanonical simulation approaches. In the first, one tries to satisfy completely the fixed-energy constraint, a typical example is the Q2R cellular automaton [24,25]. In the second, one tries to mildly relax the energy constraint by using relatively small energy windows in order to avoid ergodic problems, as done by Creutz [26] in his "demon" method. Finally, the fixed-energy constraint is completely relaxed [27] and various ideas have been tried, ranging from the tuned temperature canonical approach of Oliveira [22] to the flat histogram recipe of Wang [28].

In order to present some justification for the scheme of Eqs. (10a) and (10b) let us suppose that we know the exact DOS and we are about to perform an infinitely long entropic sampling in the restricted energy subspace (E_1,E_2). In this case we can write for the Monte Carlo process with sampling probability $P_i \propto 1/G(E)$ [4]:

$$\langle M^n\rangle = \frac{\sum_{(E_1,E_2)} \langle M^n\rangle_E G(E) e^{-\beta E}}{\sum_{(E_1,E_2)} G(E) e^{-\beta E}} \cong \frac{\sum_{i=1}^{\mathcal{N}} M_i^n P_i^{-1} e^{-\beta E}}{\sum_{i=1}^{\mathcal{N}} P_i^{-1} e^{-\beta E}} \cong \frac{\sum_{(E_1,E_2)} \langle M^n\rangle_{E,ESM} G(E) e^{-\beta E}}{\sum_{(E_1,E_2)} G(E) e^{-\beta E}}. \tag{11a}$$

The last approximation in Eq. (11a) assumes that in the limit of an infinite Markovian chain the $H_{ESM}(E)$ histogram is perfectly flat. Accordingly, $H_{ESM}(E)$ has been set equal to a constant in the denominator (in replacing the sum over the $\mathcal{N}$ sampled microstates by a sum over energies) and then moved to the numerator in order to form the ESM microcanonical averages defined by

$$\langle M^n\rangle_{E,ESM} \equiv \sum_M M^n \frac{H_{ESM}(E,M)}{H_{ESM}(E)}, \tag{11b}$$

$$H_{ESM}(E) = \sum_M H_{ESM}(E,M).$$

The above observation shows that the ESM microcanonical average should be an unbiased estimator for the fundamental microcanonical average:

$$\langle M^n\rangle_{E,ESM} \overset{\mathcal{N}\to\infty}{\longrightarrow} \langle M^n\rangle_E. \tag{12}$$

Therefore, Eq. (12) provides the essential theoretical support for using a multirange WL process (at its late stages) to obtain microcanonical simulators. It is reasonable to expect that the high-level stages ($j \gg 1$) of the WL process will resemble the dynamics of the ESM and therefore will produce good approximations for the microcanonical averages. This approach is similar in many respects to the flat-histogram method of Wang [28]. Since the resemblance of the WL process with the ESM depends on the value of the control parameter (f_j), we shall classify our recipes by using the j range utilized for updating the (E,M) histogram during the WL process. Thus, if all accepted microstates of the WL process during the j range $(j=J_{init},\ldots,J_{fin})$ are used, for updating the (E,M) histogram, the resulting recipes will be denoted by WL(J_{init}–J_{fin}). When using the N-fold version of the WL process we always start with several (J_{WL}) WL j iterations and then continue the process from the next level

($J_{N\text{-}fold}=J_{WL}+1$) by carrying out further N-fold WL iterations ($j=J_{N\text{-}fold},\ldots,J_{fin}$). In this recipe, we shall use only the N-fold iterations for updating the (E,M) histogram and time-weight the histogram by using the lifetime of microstates calculated according to the N-fold method [2,19,23]. The resulting recipes are denoted by WL(N-fold) ($J_{N\text{-}fold}-J_{fin}$).

The above described schemes were tested by using Eq. (10) to obtain certain magnetic properties of the 2D Ising model (for lattices with sizes $L=20-100$) and compare to the estimates obtained by the Metropolis method. The finite-size anomaly of the susceptibility and its value at the exact critical temperature, as well as the value of the order parameter also at the exact critical temperature were used in these tests and appear in the following subsection. For the magnetic susceptibility we have used the definition

$$\chi_L(T)=\frac{1}{N}\left(\frac{\langle M^2\rangle-\langle|M|\rangle^2}{T}\right) \tag{13}$$

and for the order parameter

$$m_T\equiv\langle|M|/N\rangle_T. \tag{14}$$

B. Metropolis versus WL-CRMES schemes: A comparative study

The estimates of the Metropolis method were obtained as follows. First an initial equilibration period of $50\times L^2$ usual Monte Carlo steps (lattice sweeps) was applied without updating the histograms. After thermalization, the updating of the histograms was applied in every Monte Carlo step, while the magnetic properties, the order-parameter distributions and the time-evolving dominant M subspaces were determined and observed in time steps of $50\times L^2$ Monte Carlo sweeps. The time evolution lasted a total of 300 such time steps for all lattice sizes (for $L=70$, 120 and 140; see also the discussion below). Thus, for a lattice of linear size $L=100$, the above time evolution accounts to a total of 1.5×10^8 lattice sweeps.

The estimates of the WL multirange process were obtained using, for each lattice size, 30 independent random walks in the appropriate (E_1,E_2) energy subspace. These subspaces were chosen carefully to cover a wide temperature range close to the critical point, so that the DOS and the $H(E,M)$ histograms produced would yield accurate estimates of all thermal and magnetic properties in the temperature range. The energy subspaces were wide enough to produce relative accuracies, within the scheme, far beyond the criterion $r=10^{-6}$, which was finally applied to determine the dominant subspaces. The time requirements of the described Metropolis estimation were notably greater than the described WL multirange process of 30 independent random walks. For $L=100$ the WL scheme was about three times faster than the Metropolis scheme. Note that the Metropolis method produces estimates only for one particular temperature and not for a wide temperature range. For a lattice of linear size $L=140$ the above described WL scheme is at least ten times faster than the described Metropolis scheme.

The estimates derived from the WL recipes appear to have relatively small deviations from the corresponding Metropolis estimates and, with a notable exception, they seem to be within the given error bounds. The comparison with the Metropolis method is presented in Figs. 4–6. The relative variations shown in these graphs are defined with respect to the Metropolis estimates by assuming that these are more accurate, i.e., we define

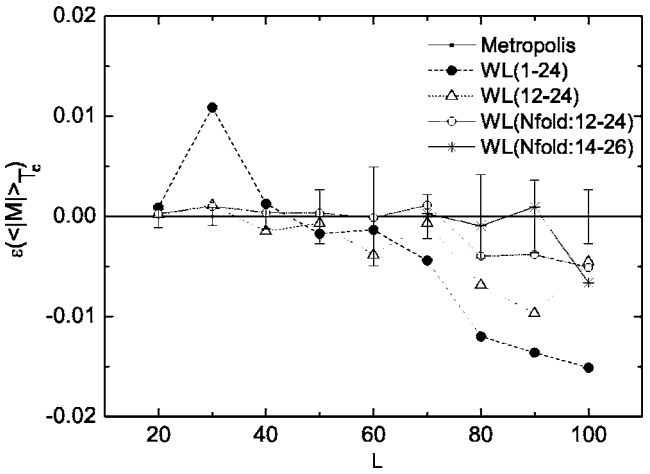

FIG. 4. Relative deviations of WL ES schemes, with respect to the Metropolis algorithm defined in Eq. (15), calculated from the order parameter at the critical temperature T_c. The error bars used show the Metropolis relative uncertainties calculated as five standard deviations in the equilibrium regime.

$$\varepsilon(Q)=\frac{Q_{\mathrm{Metr}}-Q_{WL}}{Q_{\mathrm{Metr}}} \tag{15}$$

where $Q=m_T$ and/or $Q=\chi_T$. The error bounds used in these graphs refer to the Metropolis estimates in the observed equilibrium regime which is roughly defined as the last almost flat part ($t\cong150-300$) in the above described 300 time steps. To define the error bounds we have used a confidence level

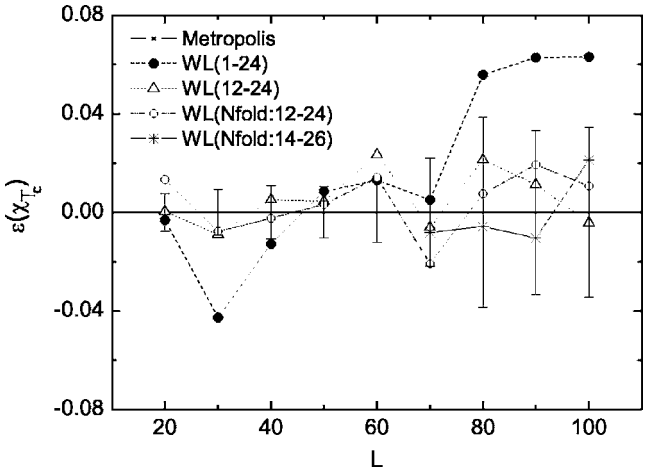

FIG. 5. The same deviations as in Fig. 4, again at T_c, calculated now from the susceptibility. The error bars as in Fig. 4 show again the Metropolis relative uncertainties calculated as five standard deviations in the equilibrium regime.

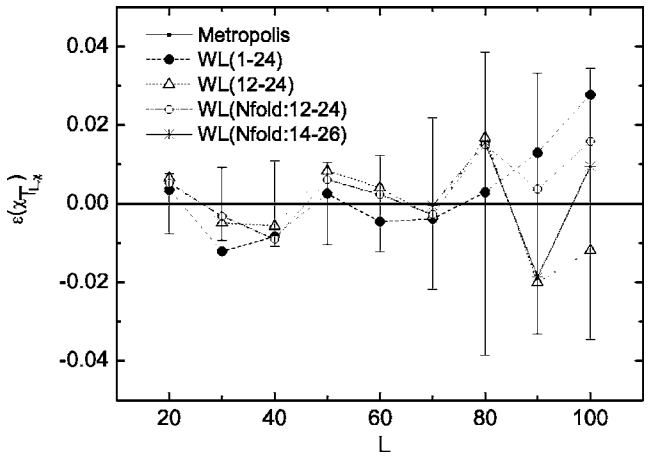

FIG. 6. Susceptibility deviations at the corresponding pseudocritical temperatures. The error bars as in Figs. 4 and 5.

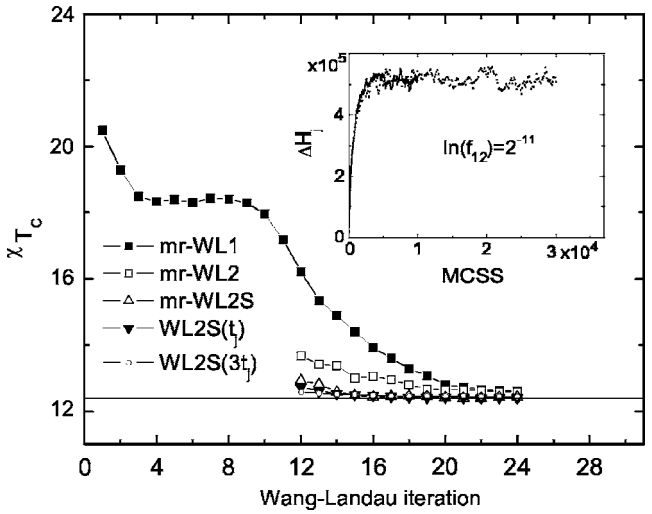

FIG. 7. Evolution of the estimates of the critical susceptibility with the WL iteration on a lattice of linear size $L=30$. The filled (open) squares present the case MR-WL1 (MR-WL2) which is the multirange WL(1–24) [WL(12–24)] recipe, described in the text. Upper open triangles (MR-WL2$\mathcal{S}$) illustrate the evolution when a separation ($\mathcal{S}$) refinement of 16 spin flips is applied between successive records in the (E,M) histograms. The last two cases WL2$\mathcal{S}(t_j)$ and WL2$\mathcal{S}(3t_j)$ (down filled triangles and open circles, respectively) correspond to a simple one-range approach of different simulation times. The duration of each WL iteration was carefully chosen, so that saturation of the histogram fluctuation was well obeyed, as shown in the inset ($j=12$). The solid line represents the estimates of χ_{T_c} obtained by the Metropolis run, as explained in the text.

of five standard deviations obtained in this wide time window.

Figure 4 shows the relative deviations from the Metropolis mean values of the order parameter at the exact critical temperature for four recipes of the WL scheme, as indicated in this figure. The Metropolis estimates have very small error bounds of the order of 0.5% or less, besides the fact that we have applied the above mentioned demanding confidence limit. The deviations of the WL schemes are reasonable (of the order of 1% or less) with the clear exception of the case WL(1–24) in which the histogram's $[H(E,M)]$ updating started from the very early stage of the WL process. For large lattices, this recipe seems to produce a significant overestimation of the order parameter, at the exact critical temperature, and this is enhanced with increasing lattice size. Since, the detailed balance is strongly violated at the early stages of the WL process, the observed failure of this recipe should be attributed to the detailed balance violation. The related overestimation may be possibly a result of an oversampling distortion of large magnetization values at the low-energy part of the energy range used. Distortions stemming from the violation of the detailed balance condition are difficult to explain and in general their origin is a subtle matter. However, such systematic distortions are not observed for the other three recipes appearing in Fig. 4. We consider this as a first strong indication that the weak violation of the detailed balance condition for these high-level WL schemes is not statistically significant. The behavior of the relative deviations for the susceptibilities at the exact critical temperature in Fig. 5, and at the pseudocritical temperatures in Fig. 6 appear in general, much better from those shown in Fig. 4. Again the distortions of the WL(1–24) scheme become pronounced as we increase the lattice size.

At this point let us try to observe in more detail the effect of the WL iteration level on an estimated magnetic property and also the effect of one of the simplest refinements of the WL algorithm for the square Ising lattice of size $L=30$. Using an accurate DOS G_{WL} obtained from a previous WL run ($J_{fin}=24$), we have calculated, with the help of Eq. (11), the critical susceptibility χ_{T_c} as a function of the WL iteration level in a new WL diffusion process. In this new multirange (MR) process each WL iteration level is repeated 30 times for each energy subinterval. Figure 7 shows the evolution of the critical susceptibility to its equilibrium value for five cases. In the first case (MR-WL1) the updating of (E,M) histograms follows the recipe WL(1–24) and in the second case (MR-WL2) the recipe WL(12–24). The third case (MR-WL2$\mathcal{S}$) follows a refinement of the WL algorithm proposed by Zhou and Bhatt [20]. The additional element of the algorithm is that now we allow for a number $\mathcal{S}$ ($\mathcal{S}=16$) spin flips between successive records in the histograms (and in the DOS modification). Introduction of such a separation diminishes systematic errors due to the correlation between adjacent records as shown in Ref. [20]. From the first case we note that starting the (E,M) histogram updating process at the early stage of the WL difusion is analogous to adding a "nonequilibrium memory effect" in our cumulative histograms. This early effect is stronger when the WL algorithm is used in a simple one-range fashion, as our simulations have shown. It is also apparent that the refinement introduced by the separation $\mathcal{S}$ clearly improves, in the cost of the additional spin flips, the behavior of the evolution of the magnetic susceptibility χ_{T_c} toward its final equilibrium value, which otherwise ($\mathcal{S}=1$) is obtained in a longer run.

Zhou and Bhatt [20] have given a proof of the convergence of the WL algorithm and found that the fluctuation of the histogram is proportional to $1/\sqrt{\ln f}$ where f is the modification factor. This has been recently confirmed by numeri-

cal tests [21], where it was shown that the criterion for reducing f goes beyond the "flat-histogram" idea and that "enough statistics" should be obtained in each WL iteration. According to Lee, Okabe, and Landau [21] an optimal algorithm will stop the simulation as soon as the histogram fluctuation at the jth iteration, denoted as $\Delta H_j = \Sigma_E [H_j(E) - \min_E \{H_j(E)\}]$, becomes saturated. In order to observe whether we will have a noticeable improvement on the magnetic susceptibility estimates by applying the proposed entropic sampling scheme [WL(12–24)] for longer simulation times, at each j (=12–24) iteration, we present also in Fig. 7 the cases WL2$\mathcal{S}(t_j)$ and WL2$\mathcal{S}(3t_j)$. Both these runs were performed via a simple one-range WL scheme, using at each iteration more Monte Carlo steps per spin (MCSS) than required for the saturation of ΔH_j. Moreover, the latter case uses three times the number of MCSS of the former. The inset of Fig. 7 illustrates the clear saturation of $\Delta H_{j=12}$ for these runs [the solid (dotted) line corresponds to duration t_j $(3t_j)$]. Comparing the estimates of the last three cases shown in Fig. 7 ($\mathcal{S}=16$) we may draw the following conclusions. First, the multirange approach applied in the case MR-WL2S gives comparable estimates to those obtained from the one-range implementation of the WL scheme and second, a much longer run, such as the WL2$\mathcal{S}(3t_j)$, does not yield a noticeable improvement. It appears that an optimal and quite accurate implementation of the proposed entropic scheme can be constructed using a multirange $H(E,M)$ histogram updating process, during the high-level "well saturated" WL iterations.

The recent combination of Lee's entropic sampling with the WL algorithm presented in Ref. [21] may be also implemented to test and possibly improve the CRMES entropic scheme proposed here. Finally, the adaptive algorithm of Trebst *et al.* [29] is of particular interest for a CRMES implementation and would also be stimulating to compare the "bottleneck region," or region of minimum diffusivity, of this method with the dominant energy subspaces as defined in this paper. Therefore, we conclude that the high-level WL-(CRMES) schemes are reasonable alternatives to the Metropolis method. The estimates for thermodynamic parameters involving higher moments of critical distributions appear to be of the same as or even better accuracy than those corresponding to the traditional method.

C. Energy and order-parameter dominant subspaces

The energy $\widetilde{E}$ producing the maximum term in the partition function at the pseudocritical temperature of the susceptibility $T_L^*[\chi] \equiv T_{L,\chi}$ may be easily located. Thus, we may apply a minimal approximation scheme analogous to that of Eq. (5) to observe the evolution of the susceptibility maximum as we expand the energy subspaces centered around $\widetilde{E}$. Now the value of the susceptibility is used in place of the specific heat and the resulting CRMES is the subspace centered at $\widetilde{E}$ corresponding to the first member of the sequence satisfying

$$\left| \frac{\chi_L^*(\Delta_\pm)}{\chi_L^*} - 1 \right| \leqslant r. \tag{16}$$

Provided that our initial guess for (E_1, E_2) is wide enough we also obtain accurate estimates for the finite-size extension of these subspaces and we would expect that the relevant scaling variable $\Psi_\chi = (\Delta\widetilde{E})_\chi^2 / L^d$ would obey the scaling law (4). Therefore, we may restate the scaling law as

$$\Psi_\Theta \equiv \frac{(\Delta\widetilde{E})_\Theta^2}{L^d} \approx L^{\alpha/\nu} \tag{17}$$

where Θ $(\equiv \Theta_L)$ denotes the finite-size value of some thermodynamic variable close to a critical point and $(\Delta\widetilde{E})_\Theta$ is the extension for appropriately defined minimum energy subspaces. In analogy with our findings [14,15] for a diverging specific heat behavior, we expect that a diverging susceptibility and the criterion (16) will yield extensions scaling according to the above law. The alternative method described in Sec. II which employs the energy density function [see Eq. (6)] may also be used and is easier to implement.

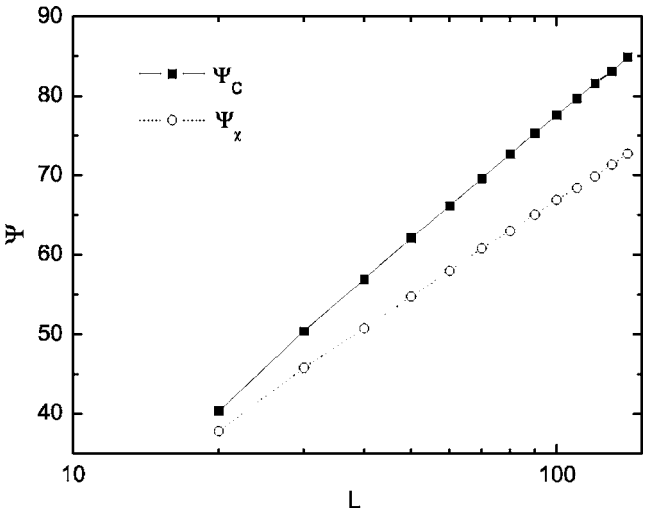

FIG. 8. 2D Ising model: Logarithmic scaling behavior of the finite-size extensions of the CRMES defined with the help of specific heat maxima according to the successive minimal approximations [Eq. (5)] and the analogous extensions of the CRMES defined with the help of the susceptibility maxima [Eq. (16)].

Figure 8 illustrates the scaling behavior of the extension of the CRMES defined with the help of the specific heat maxima [Eq. (5)] and the corresponding CRMES defined with the help of the magnetic susceptibility maxima, as discussed above [Eq. (16)]. The corresponding scaling variables should be expected to obey the scaling law (17), and for the 2D Ising model the well known logarithmic law [14,18]. As seen from this figure, this logarithmic law is well obeyed for both restrictive schemes as expected.

Finally, we may describe a procedure for specifying the dominant subspace in the order-parameter space. We assume that the energy subspace (E_1, E_2) is sufficiently broad to approximate to the desired degree of accuracy the probability density of the order parameter at some temperature of interest by

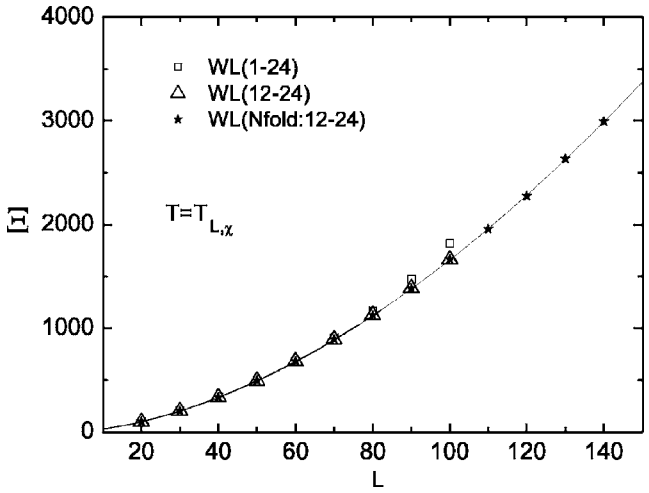

FIG. 9. 2D Ising model: Finite-size behavior of the extensions of critical minimum magnetic subspaces (CRMMSs) obtained from the WL schemes, at the susceptibility pseudocritical temperatures, calculated with the help of the definition (19) and using $r=10^{-6}$. The fitted line correspond to the power law $0.525L^{1.75}$.

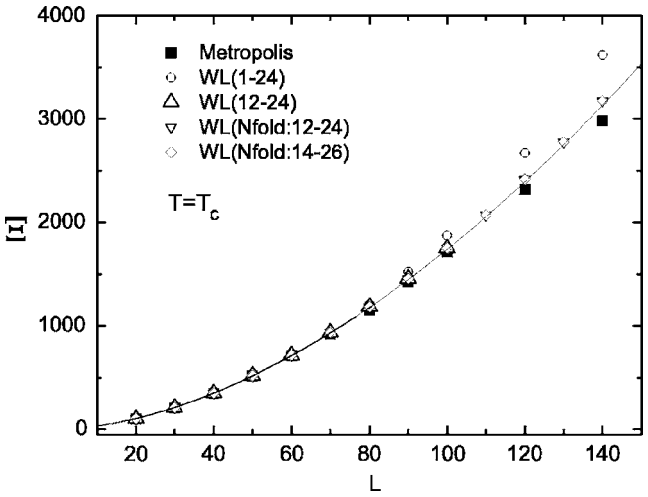

FIG. 10. The same as in Fig. 8 at the exact critical temperature T_c, including now for comparison the CRMMS corresponding to the order-parameter probability distributions obtained by the Metropolis algorithm. The fitted line, used as a guide to the eye, is the power law $0.55L^{1.75}$, obtained by fixing the exponent to 1.75 and fitting the data $L=20-140$ of the WL(N-fold:12–24) scheme. Note the decline of the Metropolis CRMMS.

$$P_T(M) \cong \frac{\sum_{E\in(E_1,E_2)} [H_{WL}(E,M)/H_{WL}(E)]G_{WL}(E)e^{-\beta E}}{\sum_{E\in(E_1,E_2)} G_{WL}(E)e^{-\beta E}}. \tag{18}$$

Next, we find the value $\tilde{M}$ that maximizes the above density, at the pseudocritical temperature $T_{L,\chi}$ (or some other temperature, for instance the exact critical temperature), and we locate the end points ($\tilde{M}_\pm$) of the magnetic critical subspaces by

$$\tilde{M}_\pm: \quad \frac{P_{T_{L,\chi}}(\tilde{M}_\pm)}{P_{T_{L,\chi}}(\tilde{M})} \leqslant r. \tag{19}$$

The above condition is in full analogy with that of Eq. (6) applied there in the energy space and since we will now consider only dominant M subspaces, defined with the help of the above probability density criterion, we shall avoid in our notation the explicit reference to the probability density. Accordingly, we denote the extension of the resulting magnetic subspaces by

$$(\Delta\tilde{M})_{T_{L,\chi}} \equiv (\Delta\tilde{M})_{P_{T_{L,\chi}}(M)} \equiv \min(\tilde{M}_+ - \tilde{M}_-), \tag{20}$$

and we should now look for a scaling law of the form

$$\Xi_{T_{L,\chi}} \equiv \Xi_{P_{T_{L,\chi}}(M)} \equiv \frac{(\Delta\tilde{M})^2_{T_{L,\chi}}}{L^d} \approx L^{\gamma/\nu}. \tag{21}$$

Figure 9 illustrates the scaling behavior of the critical minimum magnetic subspaces (CRMMSs) obtained using the magnetic space restriction (19), defined above, and the accuracy level $r=10^{-6}$ at the pseudocritical temperatures of the susceptibilities. The behavior of the high-level WL recipes is very good and provides quite accurate estimates for the critical exponent γ/ν. The line shown is the power law $0.525L^{1.75}$ which is obtained by fixing the exponent to 1.75 and fitting the WL(N-fold:12–24) data. This is almost identical with the power law obtained by using the exponent as a free parameter, which yields $0.535L^{1.746}$. Note that the deviations of the WL(1–24) scheme are not observable for small lattices. However, with increasing lattice size ($L>60$) they become quite apparent. Figure 10 presents a similar illustration at the exact critical temperature comparing now not only the WL recipes but also the Metropolis method. The deviations from the expected scaling law are now quite apparent not only for the "bad" WL(1–24) recipe but also for the Metropolis method. Table I gives estimates of the critical exponent obtained from the schemes shown in Fig. 10 using only the intermediate data $L=50-100$ in which these deviations are still moderate. From this table the overestimation of the WL(1–24) scheme but also the tendency of underestimation of the Metropolis scheme is quite obvious. The Metropolis data used for $L=20-100$ were obtained from the CRMMS developed at the end of the 300 time steps described in Sec. III B. It is of some interest to list here some details of the end points of the dominant magnetization subspaces. Let us consider the case $L=100$ as an example. The broad energy range used in our runs for the WL process was ($ie=850$, $ie=2150$), where the counting of energy states is given by $ie=(E+2N)/4+1$. The dominant energy ranges are

TABLE I. $\Xi=(\Delta M)^2/L^2 \simeq aL^w$; exact $w=\gamma/\nu=1.75$. Data fitted: $L=50-100$, $T=T_c$.

	Metropolis	WL(1–24)	WL(12–24)	WL(N-fold:14–26)
a	0.59(6)	0.31(9)	0.54(1)	0.54(1)
w	1.73(2)	1.89(6)	1.76(1)	1.76(1)

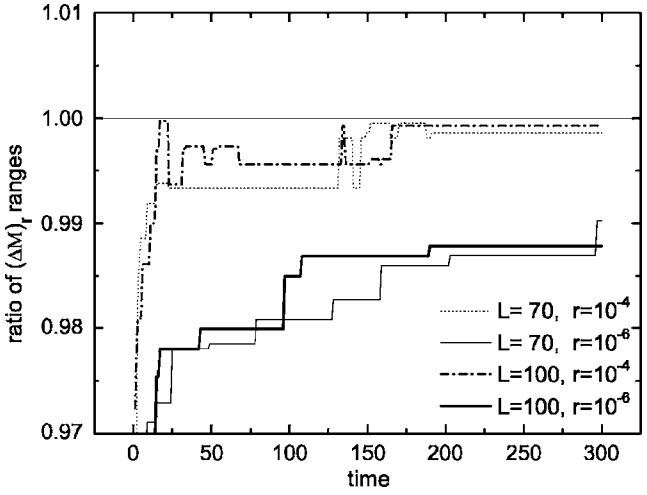

FIG. 11. Illustration of the very slow equilibration of the Metropolis algorithm in the tail regime. Time development of the extensions of CRMMS (corresponding to $r=10^{-4}$ and 10^{-6}) of the Metropolis algorithm. To observe the distance from the true or tail equilibrium we have divided the time-developing Metropolis extensions by the corresponding extensions of the WL(N-fold:12–24) scheme so that true equilibrium occurs at the value 1. It is obvious that for small r and large L true equilibrium of the Metropolis method is not attained, even for very long runs.

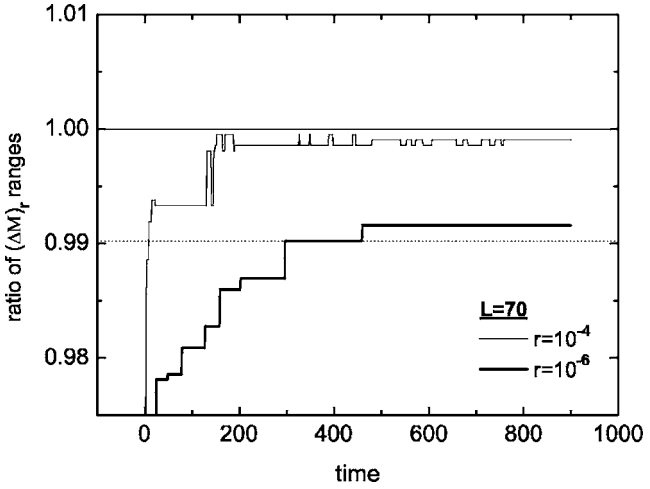

FIG. 12. The same as in Fig. 11 for $L=70$ for a longer run. The dotted line shows the maximum value obtained for $r=10^{-6}$ for the first 300 time steps (compare with Fig. 11).

(a) at the pseudocritical temperature of the specific heat [*ie* $=1061(3)$, *ie*$=1947(3)$] and (b) at the pseudocritical temperature of the susceptibility [*ie*$=1142(3)$, *ie*$=1959(3)$]. The maximum value of the magnetization sampled in the process was $|M|/N=0.912$ and the minimum value $|M|/N=0$. Defining the dominant magnetization space with the help of Eq. (19) at the pseudocritical temperature of the susceptibility, we locate this subspace as ($|M|/N=0$, $|M|/N=0.816$). This shows that the dominant magnetization subspace so defined is a subset of the sampled values. Note that for all lattice sizes the left end of the dominant magnetization subspace is $|M|/N=0$.

Let us now present the Metropolis time evolution of the dominant M subspaces since this development offers a didactic example of the very slow tail convergence of the traditional importance sampling methods. Figure 11 illustrates the slow equilibration process of the Metropolis algorithm at the tails of the order-parameter distribution. To draw this graph the time-developing CRMMS, for the two r levels ($r=10^{-4}$ and 10^{-6}) shown, was divided by the corresponding CRMMS predicted by the high-level WL(N-fold:12–24) scheme which appear to have very small errors for the lattice sizes shown. Thus, considering these later CRMMSs as exact, the Metropolis relative dominant M subspaces should grow in time toward the value 1. For the value $r=10^{-4}$ this is almost achieved at the time $t=150$ for both lattices shown, $L=70$ and 100. However, for $r=10^{-6}$, we observe a very slow relaxation process which persists even if we increase the observation time. This is obvious in Fig. 12 where, for the smaller lattice $L=70$, the time duration of the process has been increased up to $t=900$. Note that, if one was observing the equilibration process of the algorithm with respect to the mean value of the order parameter, he would then have been convinced that equilibrium of this quantity has been attained well before the time $t=150$.

This situation is due to the very slow equilibration at the tails of the distribution and in particular at the large-M tail. In fact the time expansion of the CRMMS in the Metropolis process is due to the gradual movement of the right end of the magnetization range to larger values, since the left end is $|M|/N=0$ from the very first stages of the process. Returning to the large-M range is a rare event for the Metropolis algorithm and this makes this traditional scheme inaccurate in the far tail regime, but also very inefficient for the study of the tails of the critical distributions. The data points $L=120$ and 140 for the Metropolis algorithm included in Fig. 10 were obtained by using runs with approximately equal time requirements (about 40 h in a Pentium IV 3 GHz) with the WL(N-fold:14–26) scheme. For the case $L=140$ this corresponds to only 30 time steps with the developing relative CRMMS ($r=10^{-6}$) having hardly approached the value of 0.97 only. Even by using a much longer run (for instance 100 times longer) the Metropolis algorithm will not give an adequate description of the far-tail regime.

IV. CONCLUDING REMARKS

Critical dominant energy and order-parameter subspaces can be defined by various alternative restrictive schemes, as shown in this work. In this way it is possible to optimize the Monte Carlo schemes and study simultaneously all finite-size anomalies of statistical models. The finite-size extensions of the dominant energy and order-parameter subspaces scale with exponents α/ν and γ/ν, respectively. Our experience with this subject leads us to conclude that the extensions of these dominant subspaces are more accurate than the estimates of the corresponding thermodynamic variables (specific heat and susceptibility), establishing the critical minimum subspace method as an alternative for the estimation of the associated critical exponents from finite-size Monte Carlo data.

The presented clarification and generalization of the CRMES method greatly speeds up the Monte Carlo simulations in many applications of the methods determining the spectral densities in classical statistical models. Furthermore, the presented one-run high-level WL entropic sampling schemes provide efficient alternatives when carried out in appropriately defined dominant subspaces. We expect that for complex systems with long trapping times, these schemes will appear to be much more advantageous in almost all respects. This last expectation has been verified by our studies of the random-field Ising model, which will be published shortly. Moreover, these methods have general advantages, the most important of these being (a) the fact that one can improve the $H(E,M)$ histograms by repeated application of the method (at the same time we improve the accuracy of the DOS in the energy space), and (b) the fact that their implementation in a sufficiently broad energy subspace provides data for calculating all finite-size properties of the statistical system, which are relevant for the prediction of the asymptotic critical behavior. Overall, we envisage that our study can be further utilized in many ways for the investigation of the critical behavior of statistical models in future research.

ACKNOWLEDGMENT

This research was supported by the Special Account for Research Grants of the University of Athens under Grant No. 70/4/4071.

[1] N. Metropolis, A. W. Rosenbluth, M. N. Rosenbluth, A. H. Teller, and E. Teller, J. Chem. Phys. **21**, 1087 (1953).
[2] A. B. Bortz, M. H. Kalos, and J. L. Lebowitz, J. Comput. Phys. **17**, 10 (1975).
[3] K. Binder, Rep. Prog. Phys. **60**, 487 (1977).
[4] M. E. J. Newman and G. T. Barkema, *Monte Carlo Methods in Statistical Physics* (Clarendon Press, Oxford, 1999).
[5] D. P. Landau and K. Binder, *A Guide to Monte Carlo Simulations in Statistical Physics* (Cambridge University Press, Cambridge, U.K., 2000).
[6] P. Dayal, S. Trebst, S. Wessel, D. Würtz, M. Troyer, S. Sabhapandit, and S. N. Coppersmith, Phys. Rev. Lett. **92**, 097201 (2004).
[7] J. Lee, Phys. Rev. Lett. **71**, 211 (1993).
[8] B. A. Berg and T. Neuhaus, Phys. Rev. Lett. **68**, 9 (1992).
[9] A. R. Lima, P. M. C. de Oliveira, and T. J. P. Penna, J. Stat. Phys. **99**, 691 (2000).
[10] M. Kastner, M. Promberger, and J. D. Munoz, Phys. Rev. E **62**, 7422 (2000).
[11] J.-S. Wang and R. H. Swendsen, J. Stat. Phys. **106**, 245 (2002); J.-S. Wang, T. K. Tay, and R. H. Swendsen, Phys. Rev. Lett. **82**, 476 (1999).
[12] F. Wang and D. P. Landau, Phys. Rev. Lett. **86**, 2050 (2001); Phys. Rev. E **64**, 056101 (2001).
[13] D. P. Landau and F. Wang, Braz. J. Phys. **34**, 354 (2004).
[14] A. Malakis, A. Peratzakis, and N. G. Fytas, Phys. Rev. E **70**, 066128 (2004).
[15] S. S. Martinos, A. Malakis, and I. A. Hadjiagapiou, Physica A **352**, 447 (2005).
[16] M. S. S. Challa, D. P. Landau, and K. Binder, Phys. Rev. B **34**, 1841 (1986).
[17] K. Binder and D. P. Landau, Phys. Rev. B **30**, 1477 (1984).
[18] A. E. Ferdinand and M. E. Fisher, Phys. Rev. **185**, 832 (1969).
[19] A. Malakis, S. S. Martinos, I. A. Hadjiagapiou, and A. S. Peratzakis, Int. J. Mod. Phys. C **15**, 729 (2004).
[20] C. Zhou and R. N. Bhatt, Phys. Rev. E **72**, 025701(R) (2005).
[21] H. K. Lee, Y. Okabe, and D. P. Landau, e-print cond-mat/0506555.
[22] P. M. C. de Oliveira, Braz. J. Phys. **30**, 195 (2000).
[23] B. J. Schulz, K. Binder, and M. Muller, Int. J. Mod. Phys. C **13**, 477 (2001).
[24] Y. Pomeau, J. Phys. A **17**, 415 (1984); G. Vichniac, Physica D **10**, 96 (1984).
[25] H. J. Herrmann, J. Stat. Phys. **45**, 145 (1986); J. G. Zabolitzky and H. J. Herrmann, J. Comput. Phys. **76**, 426 (1988).
[26] M. Creutz, Phys. Rev. Lett. **50**, 1411 (1983).
[27] B. Berg, Nature (London) **361**, 708 (1993).
[28] J.-S. Wang, Eur. Phys. J. B **8**, 287 (1999); Physica A **281**, 147 (2000).
[29] S. Trebst, D. A. Huse, and M. Troyer, Phys. Rev. E **70**, 046701 (2004).